One-step induction of photoreceptor-like cells from human iPSCs by delivering transcription factors

AUTHOR(S):

Otsuka, Yuki; Imamura, Keiko; Oishi, Akio; Kondo, Takayuki; Suga, Mika; Yada, Yuichiro; Shibukawa, Ran; ... Tsukita, Kayoko; Tsujikawa, Akitaka; Inoue, Haruhisa

CITATION:

Otsuka, Yuki ...[et al]. One-step induction of photoreceptor-like cells from human iPSCs by delivering transcription factors. iScience 2022, 25(4): 103987.

ISSUE DATE:

2022-04

URL:

http://hdl.handle.net/2433/269077

iScience

CellPress OPEN ACCESS

Article

One-step induction of photoreceptor-like cells from human iPSCs by delivering transcription factors

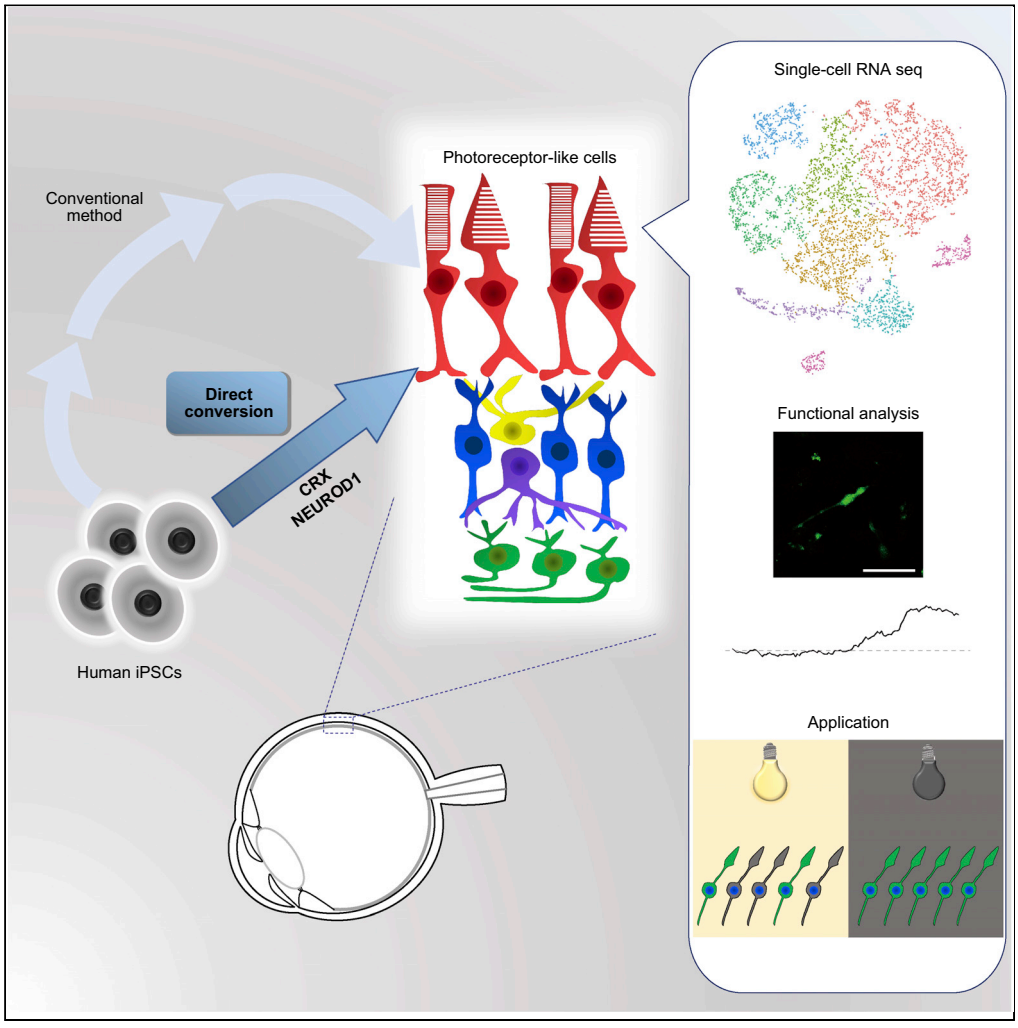

Yuki Otsuka, Keiko Imamura, Akio Oishi, ..., Kayoko Tsukita, Akitaka Tsujikawa, Haruhisa Inoue

haruhisa.inoue@riken.jp

Highlights

Introduction of CRX and NEUROD1 to iPSCs generated photoreceptor-like cells

Generated photoreceptor-like cells expressed phototransduction-associated genes

Generated photoreceptor-like cells exhibited functional property

Light-induced damage models were constructed using photoreceptor-like cells

Otsuka et al., iScience 25, 103987
April 15, 2022
https://doi.org/10.1016/j.isci.2022.103987

iScience

CellPress OPEN ACCESS

Article

One-step induction of photoreceptor-like cells from human iPSCs by delivering transcription factors

Yuki Otsuka,[1,2,3] Keiko Imamura,[1,2,4] Akio Oishi,[3] Takayuki Kondo,[1,2,4] Mika Suga,[1,2] Yuichiro Yada,[1,2] Ran Shibukawa,[1,2] Yasue Okanishi,[1] Yukako Sagara,[1] Kayoko Tsukita,[1,2] Akitaka Tsujikawa,[3] and Haruhisa Inoue[1,2,4,5,*]

SUMMARY

Retinal dystrophies (RDs) lead to irreversible vision impairment with no radical treatment. Although photoreceptor cells (PRCs) differentiated from human induced pluripotent stem cells (iPSCs) are essential for the study of RDs as a scalable source, current differentiation methods for PRCs require multiple steps. To address these issues, we developed a method to generate PRCs from human iPSCs by introducing the transcription factors, CRX and NEUROD1. This approach enabled us to generate induced photoreceptor-like cells (iPRCs) expressing PRC markers. Single-cell RNA sequencing revealed the transcriptome of iPRCs in which the genes associated with phototransduction were expressed. Generated iPRCs exhibited their functional properties in calcium imaging. Furthermore, light-induced damage on iPRCs was inhibited by an antioxidant compound. This simple approach would facilitate the availability of materials for PRC-related research and provide a useful application for disease modeling and drug discovery.

INTRODUCTION

The retina, a photosensitive tissue, lines the inner surface of the eye and conveys visual information to the brain via optic nerve. Photoreceptor cells (PRCs), one of the retinal components, are primary light-sensing cells. They convert light information to electrical signals that are relayed to the brain through several interneurons (Singh et al., 2018). Retinal dystrophies (RDs) are a diverse group of diseases characterized by progressive degeneration of PRCs leading to irreversible vision loss and are major causes of blindness affecting more than 4.5 million patients worldwide (Hohman, 2016). Several treatment approaches for RDs including pharmacological agents (Hasegawa et al., 2018), retinal prosthesis (Ayton et al., 2020), gene therapy (Diakatou et al., 2019), and cell transplantation (Tu et al., 2019) have shown potential during the recent decade. However, they are still challenging, and there are no radical treatments for RDs.

Retinal biopsies are invasive and virtually inaccessible (Milam et al., 1998); therefore, histopathologic analysis of RDs are limited to postmortem eyes. Thus, investigating the pathological process of the disease, especially in the early stage is difficult. The technology of induced pluripotent stem cells (iPSCs) enabled the generation of retinal cells and *in vitro* models to study these diseases (Takahashi and Yamanaka, 2006). Several differentiation methods to generate PRCs have been reported. In particular, three-dimensional (3D) retinal organoids have been used, showing the expression patterns of targeted cell-specific markers and being adopted for the modeling of RDs (Megaw et al., 2017; Parfitt et al., 2016; Schwarz et al., 2017). However, these methods require multiple steps and longtime culture to generate PRCs with a limited number of targeted cells (Deng et al., 2018; Wahlin et al., 2017).

In addition to the 3D organ culture technique, direct reprogramming technology has been developed for various tissues. Using this method, somatic cells are converted into sought-for lineages through the forced expression of lineage-determining factors (Duran Alonso et al., 2018; Graf and Enver, 2009; Zhou et al., 2008). This approach has already been reported in the generation of retinal pigment epithelium (RPE) (Zhang et al., 2014) or corneal epithelial cells (Cieślar-Pobuda et al., 2016; Kitazawa et al., 2019) from human

[1]iPSC-based Drug Discovery and Development Team, RIKEN BioResource Research Center, Kyoto, Japan

[2]Center for iPS Cell Research and Application (CiRA), Kyoto University, Kyoto, Japan

[3]Department of Ophthalmology and Visual Sciences, Kyoto University Graduate School of Medicine, Kyoto, Japan

[4]RIKEN Center for Advanced Intelligence Project (AIP), Kyoto, Japan

[5]Lead contact

*Correspondence: haruhisa.inoue@riken.jp

https://doi.org/10.1016/j.isci.2022.103987

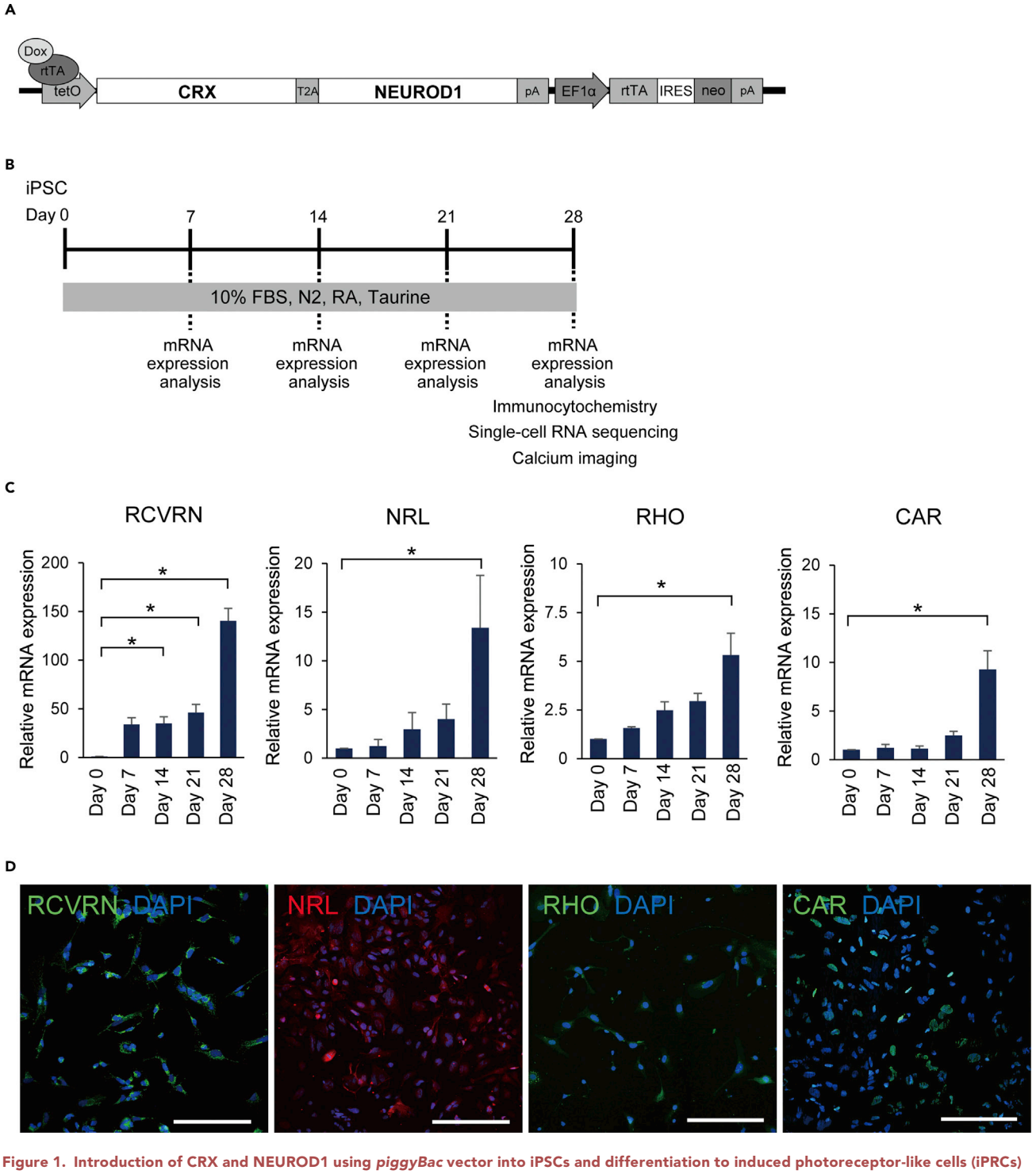

Figure 1. Introduction of CRX and NEUROD1 using *piggyBac* vector into iPSCs and differentiation to induced photoreceptor-like cells (iPRCs)

(A) Design of polycistronic *piggyBac* vector for CRX and NEUROD1 mediated conversion under control of the tetracycline operator rtTA and neomycin resistance gene. Dox: doxycycline, rtTA: reverse tetracycline transactivator, *neo*: neomycin resistance gene.

(B) Outline shows experimental procedures depending on the culture periods of iPRCs differentiation. Quantitative PCR analysis was conducted on day 7, 14, 21, and 28. Immunocytochemistry, single-cell RNA sequencing, and calcium imaging were performed on day 28. Culture medium containing DMEM/F12 - Glutamax, 1% N2 supplement, 10% Fetal Bovine Serum, 0.5 μM Retinoic acid, and 0.1 mM taurine was used throughout the differentiation. Doxycycline was removed from the medium three days before all analyses.

Figure 1. *Continued*

(C) Quantitative PCR analyses of iPSCs (Clone 1) and iPRCs cultured for 7, 14, 21, 28 days, respectively, with a photoreceptor precursor marker (RCVRN), rod cell markers (NRL and RHO), and a cone cell marker (CAR) are shown. The vertical axis indicates the expression levels of each gene, relative to human iPSCs described as Day 0. One-way ANOVA was used for statistical comparison (*$p < 0.05$). Error bars show SEM (n = 3) of biological triplicates.

(D) Representative immunofluorescence images of iPRCs on day 28 with photoreceptor markers including RCVRN, NRL, RHO, and CAR. Scale bars, 200 μm.

dermal fibroblasts. Especially, it has been attempted to generate PRCs from iris-derived cells (Seko et al., 2012), dermal fibroblasts (Fukuda et al., 2018; Seko et al., 2014), and peripheral blood mononuclear cells (PBMCs) (Komuta et al., 2016), showing the expression of PRC markers. However, these approaches exhibited limited scalability because somatic cells are not infinite in number.

To address these issues, we developed a method to generate PRCs from human iPSCs by introducing transcription factors. We evaluated the characteristics of generated cells and optimized the culture condition. The protocol enables reproducible generation of PRCs from iPSCs with an efficient number and would be beneficial for the development of RD models.

RESULTS

Generation of photoreceptor-like cells from human iPSCs using transcription factors

We developed a photoreceptor differentiation method by transducing two transcription factors, cone-rod homeobox (CRX) and neuronal differentiation 1 (NEUROD1), into human iPSCs. These genes were selected based on a previous report that identified CRX and NEUROD1 as essential factors for photoreceptor induction from iris-derived cells (Seko et al., 2012). A polycistronic vector containing CRX and NEUROD1 under control of the tetracycline operator was introduced to iPSCs using a *piggyBac* vector, which was randomly inserted in the genome (Figure 1A). After neomycin selection, the iPSCs with the vector construct were established as stable iPSC clones. We cultured these iPSCs with doxycycline and found that differentiated cells expressing Recoverin (RCVRN) were generated from iPSCs within 14 days. We defined these cells obtained by this direct conversion protocol as induced photoreceptor-like cells (iPRCs).

To evaluate the expression of molecular markers for PRCs, we cultured iPRCs until day 28 and conducted qPCR analysis on day 7, 14, 21, and 28 (Figure 1B). The expression of RCVRN was significantly upregulated in just 14 days and that it was further enhanced on day 28. Meanwhile, increased mRNA expression of neural retina-specific leucine zipper (NRL), rhodopsin (RHO), and cone arrestin (CAR) was observed on day 28 (Figure 1C). Immunocytochemistry (ICC) was performed on day 28 to confirm the immunostaining of each PRC marker with iPRCs (Figure 1D). The differentiation rates of RCVRN-positive, NRL-positive, RHO-positive, and CAR-positive cells were 34.4 ± 3.7%, 21.8 ± 1.4%, 2.9 ± 0.7%, and 18.1 ± 0.5%, respectively (mean ± SEM, n = 3). These results indicated that photoreceptor precursors expressing RCVRN were produced within 14 days and both rod and cone cell differentiation continued to progress from day 14–28.

To evaluate the reproducibility of the direct conversion method, we differentiated two other iPSC clones and one embryonic stem cell (ESC) clone for 28 days and performed immunostaining with photoreceptor markers and the percentages of photoreceptor marker-positive cells were analyzed. We confirmed similar differentiation rates were obtained in each marker with three different healthy iPSCs and ESCs (Figure S1A and S1B). In this way, we succeeded in producing photoreceptor-like cells from human iPSCs by the introduction of CRX and NEUROD1.

Single-cell RNA sequencing of generated cells

Subsequently, single-cell RNA sequencing (scRNA-seq) was conducted to reveal the transcriptome of iPRCs on day 28. Seven groups of transcriptomically similar cells were identified (Figure 2A). Photoreceptor cell-specific markers (NRL and GNB3; encoding cone G protein subunit beta 3) (Arno et al., 2016)-positive cells were detected in cluster 3 (Figure 2B)). Furthermore, the expression of genes regulating photoreceptor specification and those encoding molecules associated with phototransduction were not only dominantly identified in cluster 3 but also in other clusters (Figures 2C and S2A); NRL and nuclear receptor subfamily 2 group E member 3 (NR2E3) play a role in rod specification, and retinoid X receptor gamma (RXRG) is a key regulator for cone differentiation (Swaroop et al., 2010). Important components in the phototransduction cascade in both rod and cone photoreceptor cells include G protein subunit gamma transducin 1 (GNGT1) and G protein subunit beta 3 (GNB3) encoding G protein transducin subunit in rod and cone cells, respectively, and phosphodiesterase 6A (PDE6A) and phosphodiesterase 6H (PDE6H) encoding

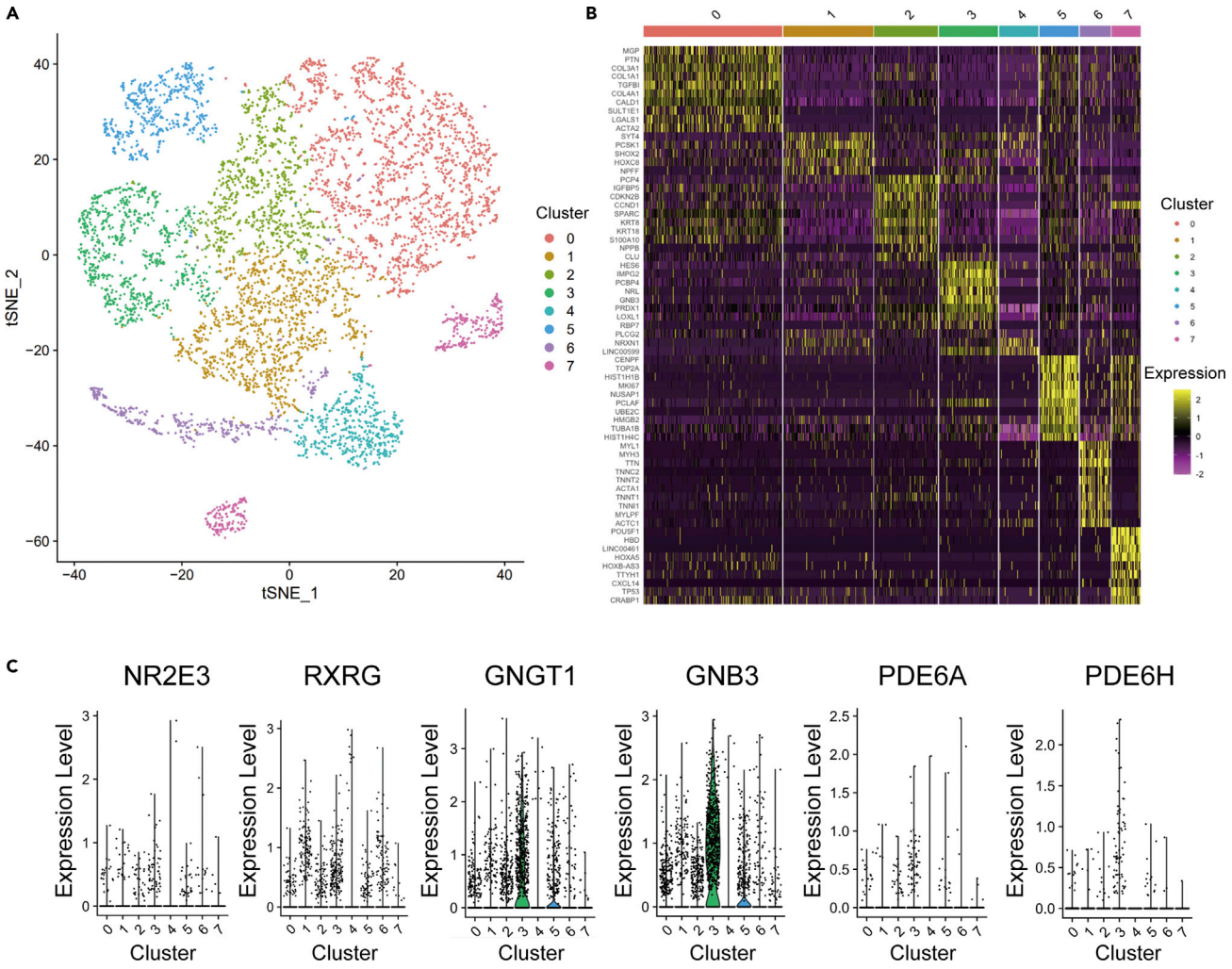

Figure 2. Single-cell RNA sequencing of generated cells

(A) tSNE plot shows the infomap clusters with iPRCs on day 28. Each point represents the transcriptome of a single cell.

(B) Highly expressed genes (row) in each cluster (column) are shown.

(C) The expression levels of representative photoreceptor cell markers in individual cells in each cluster are presented. Each point represents the transcriptome of a single cell in each cluster.

phosphodiesterase in rod and cone cells, respectively (Figure 2C). Therefore, we found that many retinal disease-related genes, most of which are crucial to photoreceptor functions, were expressed in the generated cells on day 28.

Meanwhile, differentiated cells expressing representative Horizontal cell markers (one cut homeobox 1 (ONECUT1) and LIM homeobox 1 (LHX1)) or Amacrine cell markers (transcription factor AP-2 (TFAP2) and glutamate decarboxylase 2 (GAD2)) were dominantly identified in cluster 7 (Figure S2B).

iPRCs-contained functional cyclic nucleotide-gated (CNG) cationic channels

Calcium imaging was performed to examine whether iPRCs contained the functional machinery necessary for phototransduction. We tested their ability to exhibit an inward dark current corresponding to an influx of sodium (Na^+) and calcium (Ca^{2+}) via cyclic nucleotide-gated (CNG) cationic channels by a membrane-permeant cGMP analogue (8-Br-cGMP), as previously described (Mellough et al., 2015) (Reichman et al., 2017). Ca^{2+} indicator Fluo-8 was loaded to iPRCs on day 28 and its influx was monitored with live confocal imaging. When exposed to 8-Br-cGMP, some of the Fluo-8-loaded iPRCs showed Ca^{2+} influx with increased intracellular fluorescence (Figures 3A and 3B). The average fluorescence variation during the

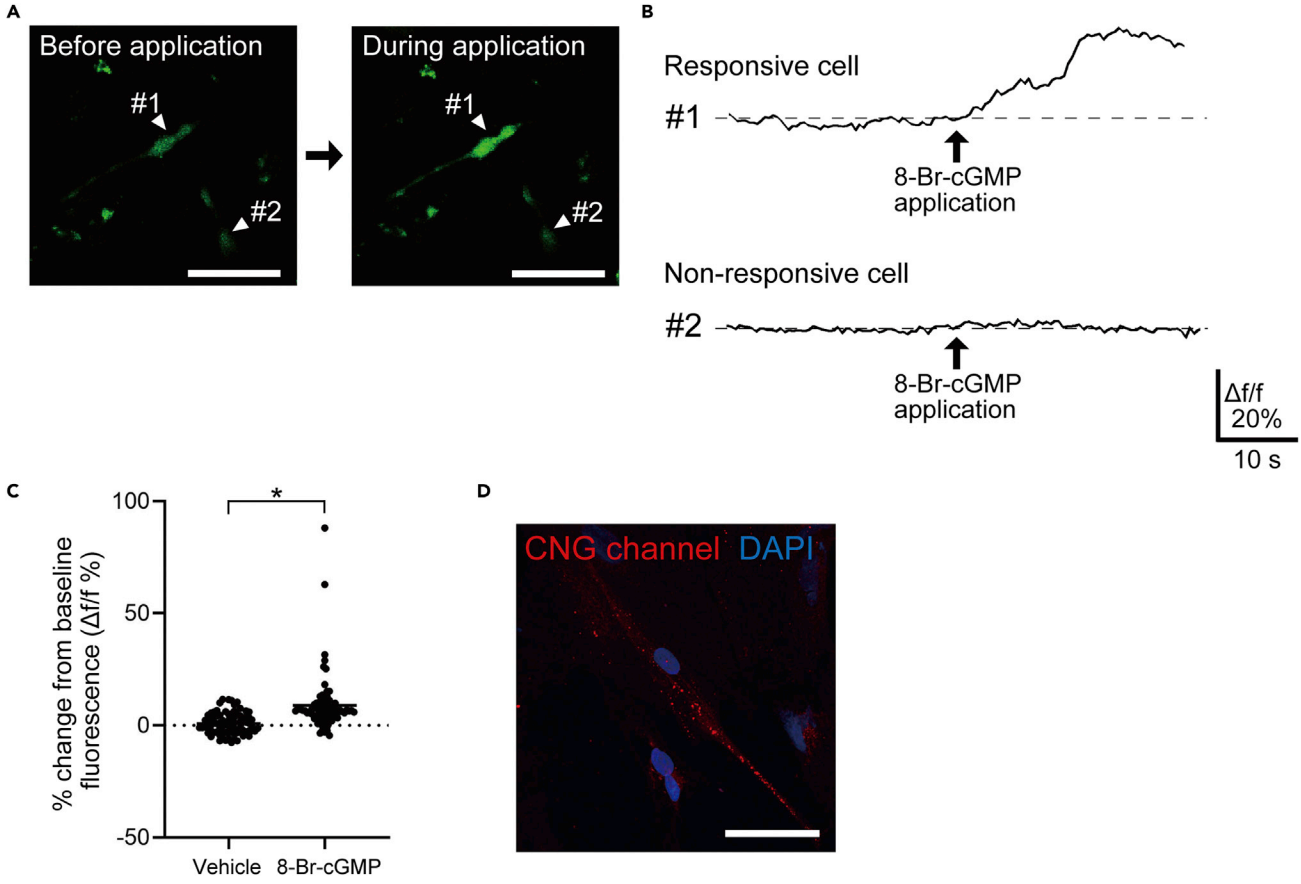

Figure 3. Calcium imaging with induced photoreceptor-like cells (iPRCs) on day 28

(A) Representative confocal images of Fluo-8-AM-loaded induced photoreceptor-like cells (iPRCs) before (left) and during (right) cGMP analogue (8-Br-cGMP) application. White arrowheads indicate a responsive cell (#1) and a non-responsive cell (#2), respectively. Scale bars, 50 μm.

(B) The raw traces of fluorescence intensity are displayed. The numbers correspond to those in Figure 4A. iPRC #1 exhibited approximately 31.1% of increase in intracellular fluorescence by 8-Br-cGMP exposure, whereas iPRC #2 did not show a significant change.

(C) The dot plot represents the average of each change in fluorescence intensity by the addition of the vehicle or 8-Br-cGMP. Eighty iPRCs were randomly picked up from three independent experiments. Unpaired *t*-test was used for statistical comparison (*$p < 0.05$).

(D) Immunostaining of cyclic nucleotide-gated (CNG) cationic channels was observed in iPRCs. Scale bar, 50 μm.

recording of eighty iPRCs was 8.5 ± 1.5% and it was significantly larger than the change induced by vehicle injection (0.33 ± 0.49%) (Figure 3C). In particular, several iPRCs exhibited robust Ca^{2+} influx, showing more than 30% change from baseline fluorescence. We also performed ICC for the CNG channel and confirmed its staining (Figure 3D).

scRNA-seq analysis detected the expression of CNGs in iPRCs (Figure S2A). CNGA1 forms a heterotetramer with CNGB1 in rod photoreceptors, whereas CNGA3 and CNGB3 are expressed in cone photoreceptors (Podda and Grassi, 2014). The intensity changes in fluorescence depend on the expression levels and the combinations of any of CNGA1, CNGB1, CNGA3, or CNGB3 expressions (Komuta et al., 2016). These results demonstrated that iPRCs presented the functional property with CNG cationic channels.

Light-induced cell damage was inhibited by an antioxidant compound

To apply iPRC to study photoreceptor diseases, we constructed a light-induced phototoxicity model using iPRCs (Figure 4A). On day 27, the medium was changed to one without Phenol Red to avoid light absorption and it was supplemented with 9-cis-Retinal vitamin A analog to activate the phototransduction cascade (Seko et al., 2014) (Cowan et al., 2020) (Figure 4B). One hour after compound treatment, iPRCs were exposed to white LED light for 24 hours and the number of cells expressing photoreceptor markers were evaluated with ICC. The number of RCVRN-positive cells did not differ between iPRCs cultured in the

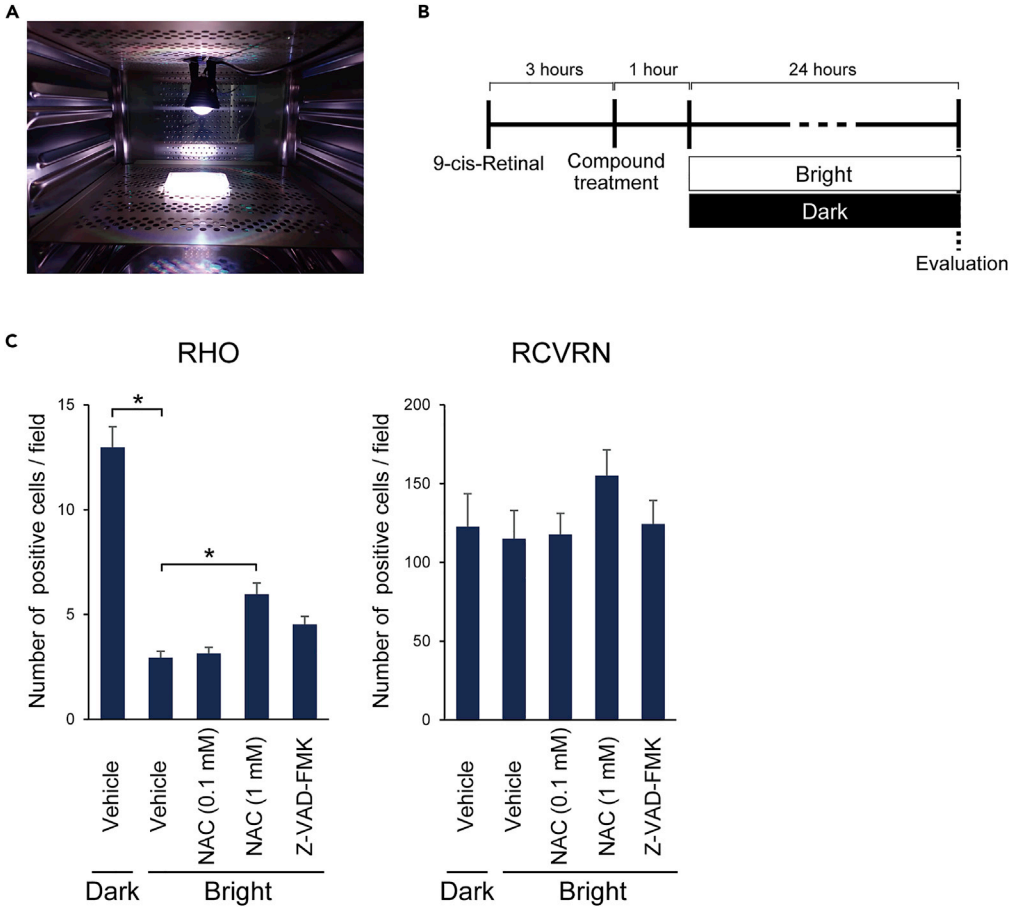

Figure 4. Effects of light on the cell viability of induced photoreceptor-like cells (iPRCs)

(A) White LED light was exposed to cells cultured in a 24-well plate at 37°C in a standard 5% CO_2 incubator.

(B) The outline shows the experimental procedures. 9-cis-Retinal vitamin A analog was supplemented 4 hours before the beginning of light stimulation. One hour after iPRCs were treated with vehicle (DMEM), N-acetylcysteine (NAC), or Z-VAD-FMK, iPRCs were exposed to white LED light for 24 hours.

(C) The number of RCVRN or RHO-positive cells per field was analyzed under each culture condition. Error bars are SEM of 36 fields. *$p < 0.05$, one-way ANOVA.

dark and under light exposure. However, the number of RHO expressing iPRCs was significantly decreased by light exposure, compared to controls cultured in a dark state (Figure 4C). Under the light condition, the loss of RHO-positive cells was inhibited by an antioxidant, 1 m M *N*-acetylcysteine (NAC) treatment, whereas 0.1 mM NAC was not effective for suppressing cell death.

3D-structure formation improved the differentiation of iPRCs

Subsequently, we investigated whether the 3D-structure formation of iPRCs promotes the photoreceptor differentiation (Figure S3A). Floating culture of iPRC bodies (FiPBs) were cultured until day 28 (Figure S3B). ICC following cryosectioning demonstrated the intriguing staining pattern of photoreceptor markers. RCVRN and RHO were diffusely distributed throughout the aggregates (Figure S3C). The percentage of positive cells for RCVRN or RHO was 44.2 $\pm$ 4.2% or 6.0 $\pm$ 0.9%, respectively (n = 8 fields from 4 FiPBs). We also conducted qPCR analysis to compare the differentiation status with adherent cultured iPRCs. Although the expression levels of RCVRN and NRL were not significantly different, the expression levels of both RHO and CAR were elevated in FiPBs, suggesting that 3D formation brought the progression of both rod and cone cell differentiations (Figure S3D). We also examined the effect of high oxygen treatment (40%), expecting further improvement of photoreceptor differentiation. FiPBs were cultured under normal or high oxygen conditions and the photoreceptor marker expression levels were compared by qPCR analysis on day 28. However, the expressions of photoreceptor markers including RHO and CAR were

Table 1. Comparison of methods for photoreceptor cell generation

	Cell source	Scalability	Transcriptional factors	Number of experimental steps	Duration to RCVRN-positive cells (days)	Reference
This study	iPSC	Unlimited	CRX, NEUROD1	1	<14	–
Conventional methods						
2D culture	iPSC	Unlimited	(–)	5	<90	Takahashi and Yamanaka (2006)
3D organoid	iPSC	Unlimited	(–)	3	50	Megaw et al. (2017) Parfitt et al. (2016) Schwarz et al. (2017)
Direct reprogramming	Iris-derived cell	Limited	CRX, NEUROD1	1	<7	Seko et al. (2012)
Direct reprogramming	Dermal fibroblast	Limited	CRX, NEUROD1, RAX, (OTX2)	1	<14	Seko et al. (2014)
Direct reprogramming	PBMC	Limited	CRX, (NEUROD1, RAX)	1	N/A	Komuta et al. (2016)
Direct reprogramming	Dermal fibroblast Fetal lung fibroblast	Limited	Five compounds	2	<10	Mahato et al. (2020)

PBMC: peripheral blood mononuclear cell.

remarkably reduced (Figure S3D). We confirmed that high oxygen concentration did not contribute to promoting the differentiation status in FiPBs.

The late steps of photoreceptor maturation take place autonomously via intrinsic factor release, whereas the addition of extrinsic compounds largely affects differentiation in the early stages (Achberger et al., 2019). Meanwhile, self-organization in 3D culture is driven via an intrinsic program of the orchestrated local cellular interactions (Nakano et al., 2012). Our findings indicated that intrinsic factor release and more robust cellular interaction probably contributed to the differentiation of FiPBs.

DISCUSSION

We developed a method to generate photoreceptor-like cells from human iPSCs by forced expression of two transcription factors. Table 1 summarizes the comparison of methods to generate PRCs. In contrast to previous direct reprogramming methods, we used iPSCs as a cell source and employed *piggyBac* transposon system. Our simple method enabled us to supply reproducible and unlimited numbers of PRCs with one step. Generated iPRCs exhibited their functional property with the expression of phototransduction-associated genes. Furthermore, they provided a useful application for disease modeling and drug discovery.

For differentiation toward PRCs, two transcription factors, CRX and NEUROD1, were introduced into iPSCs. Ectopic expression of CRX failed to produce a rod-like epigenome, suggesting that CRX is not a pioneer transcription factor that can bind to fully closed sites to induce *de novo* chromatin remodeling for cell fate specification (Ruzycki et al., 2018). In the current study, CRX and NEUROD1 were sufficient for iPSCs to differentiate to photoreceptor cells, indicating that NEUROD1 contributes to chromatin remodeling and enables CRX to bind to the promoter of rod and cone genes and activate their expression via its transactivation domain. In addition, this demonstrates that the potential tendency of iPSCs to differentiate toward PRCs is higher than that of dermal fibroblasts, because the expression of retina and anterior neural fold homeobox (RAX) is required for the induction of photoreceptors from dermal fibroblasts (Seko et al., 2014).

CRX is a homeodomain transcription factor that plays a key role in both rod and cone photoreceptor development and maintenance (Chen et al., 1997; Furukawa et al., 1997). It is described that CRX interacts with NRL for leading rod differentiation, and the cells expressing only CRX are committed to cone photoreceptor fate (Oh et al., 2007). In Crx-deficient mice, photoreceptors are generated but failed to express many phototransduction genes (Furukawa et al., 1999). In this study, scRNA-seq analysis showed crucial transcription factors for photoreceptor differentiation; in addition, a series of phototransduction molecules in both rod and cone photoreceptor cells were detected.

Meanwhile, scRNA-seq analysis also revealed that differentiated cells expressed representative markers of other retinal neuronal cells such as Horizontal or Amacrine cells. NEUROD1 has been described as a regulator of both rod (Morrow et al., 1999) and cone photoreceptors (Liu et al., 2008) during retinal development. In addition, it is primarily a pioneer transcriptional factor that plays a crucial role in neurogenesis (Egawa et al., 2020) and is involved in the determination of Horizontal and Amacrine cells (Xiang, 2013). These reports support the finding in our study that retinal cells other than photoreceptors are included in the generated cells.

The advantages of primary retinal cultures created from several mammalian donors and 3D organoids are their anatomical similarity to the human retina and that they contain other retinal cells. This can facilitate recapitulating *in vivo* development more closely and utilizing it as complex disease modeling *in vitro* (Oswald and Baranov, 2018). In contrast, photoreceptor cell lines, represented by an immortalized mouse cone photoreceptor cell, 661W do not provide an architecture of native tissue and functional influence of other retinal cell types, rather they facilitate the evaluation of isolated cells. In previous reports, 661W was used as RD models for studying light-induced damage (Kuse et al., 2015), photooxidative stress (Kanan et al., 2008), ciliopathy (Wheway et al., 2019), and other conditions. To confirm whether iPRCs are useful for such models, we evaluated light-induced cell death with iPRCs. The mechanism of retinal photoreceptor cell damage induced by light has not been fully understood yet. However, the only known common mechanism is the dependence on the Rhodopsin molecule (Joly et al., 2009) and the increase in reactive oxygen species (ROS) following light exposure is one of the major factors causing photoreceptor cell death (Dunaief, 2002). In the current study, although RCVRN-positive cells were not affected, the number of iPRCs with RHO expression was drastically decreased by light exposure. In addition, light-induced cell death was inhibited by NAC treatment. NAC was reported to protect against light-induced cellular damage by suppressing ROS generation (Kuse et al., 2015). In iPRCs, RHO was bleached by intense and persistent light stimulation and this led to several downstream mechanisms including ROS increase. In addition, because RCVRN-positive cells included more immature cells without RHO expression, significant phototoxicity was probably not observed. These results demonstrated that iPRCs generated by this simple approach would provide a useful application for disease modeling and drug discovery.

To summarize, we report a direct conversion method using transcription factors to produce photoreceptor-like cells from human iPSCs. We could obtain these cells with one step. Our simple approach significantly reduced the efforts required to generate PRCs and will provide a powerful method for diverse applications including the modeling and drug discovery of RDs.

Limitations of the study

There are some technical limitations. First, we were not able to obtain photoreceptor cells with ultrastructure including an outer segment (OS). Nevertheless, it is still difficult to generate a robust and functional OS structure by other protocols, even if the differentiation period is extended. It may be beneficial to further improve the introduced transcription factors or culture conditions for further promotion of the differentiation status. Second, iPRCs probably consist of various cells at different differentiation stages. According to previous reports, CD73, CD29, or fucosyltransferase 4 (FUT4) were suitable markers for selecting photoreceptor precursors; however, there is no effective strategy to purify more differentiated PRCs expressing RHO or cone opsins (Gagliardi et al., 2018) (Lakowski et al., 2018). In fact, transgenic Nrl-GFP mouse was used for purifying rod cells (Mahato et al., 2020). The powerful methods of purifying PRCs will facilitate this direct conversion method for its application to compound screening and other practical situations.

STAR★METHODS

Detailed methods are provided in the online version of this paper and include the following:

- KEY RESOURCES TABLE
- RESOURCE AVAILABILITY
  - Lead contact
  - Materials availability
  - Data and code availability
- EXPERIMENTAL MODEL AND SUBJECT DETAILS
  - iPS and ES cell lines and maintenance
- METHOD DETAILS
  - Preparation of a *piggyBac* vector and introduction into iPSCs

- Photoreceptor-like cell differentiation from human iPSCs
- Reverse transcription quantitative polymerase chain reaction (RT-qPCR)
- Immunocytochemistry (ICC)
- Single-cell RNA sequencing
- Calcium imaging
- Light-induced cell death analysis

- QUANTIFICATION AND STATISTICAL ANALYSIS

SUPPLEMENTAL INFORMATION

Supplemental information can be found online at https://doi.org/10.1016/j.isci.2022.103987.

ACKNOWLEDGMENTS

We thank all of our coworkers and collaborators including Takako Enami for their technical support. We acknowledge Makiko Yasui, Mikie Iijima, Nozomi Kawabata, Tomomi Urai, and Miho Nagata for their administrative support. We would like to thank Knut Woltjen for providing materials. This research was funded in part by a grant for Core Center for iPS Cell Research of the Research Center Network for Realization of Regenerative Medicine from the Japan Agency for Medical Research and Development (AMED) to H.I. and iPS Cell Research Fund.

AUTHOR CONTRIBUTIONS

H.I. and K.I. conceived the project. Y.O., R.S., Y.Okanishi, Y.S., K.T. performed the experiments. Y.O., K.I., A.O., T.K., M.S., Y.Y., A.T., and H.I. analyzed the data and provided scientific discussions. Y.O., K.I., and H.I. wrote the manuscript.

DECLARATION OF INTERESTS

The authors declare no competing interests.

Received: July 13, 2021
Revised: January 10, 2022
Accepted: February 24, 2022
Published: April 15, 2022

REFERENCES

Achberger, K., Haderspeck, J.C., Kleger, A., and Liebau, S. (2019). Stem cell-based retina models. Adv. Drug Deliv. Rev. *140*, 33–50.

Arno, G., Holder, G.E., Chakarova, C., Kohl, S., Pontikos, N., Fiorentino, A., Plagnol, V., Cheetham, M.E., Hardcastle, A.J., Webster, A.R., and Michaelides, M. (2016). Recessive retinopathy consequent on mutant G-protein β subunit 3 (GNB3). JAMA Ophthalmol. *134*, 924.

Ayton, L.N., Barnes, N., Dagnelie, G., Fujikado, T., Goetz, G., Hornig, R., Jones, B.W., Muqit, M.M.K., Rathbun, D.L., Stingl, K., et al. (2020). An update on retinal prostheses. Clin. Neurophysiol. *131*, 1383–1398.

Chen, S., Wang, Q.-L., Nie, Z., Sun, H., Lennon, G., Copeland, N.G., Gilbert, D.J., Jenkins, N.A., and Zack, D.J. (1997). Crx, a novel otx-like paired-homeodomain protein, binds to and transactivates photoreceptor cell-specific genes. Neuron *19*, 1017–1030.

Cieślar-Pobuda, A., Rafat, M., Knoflach, V., Skonieczna, M., Hudecki, A., Małecki, A., Urasińska, E., Ghavami, S., and Łos, M.J. (2016). Human induced pluripotent stem cell differentiation and direct transdifferentiation into corneal epithelial-like cells. Oncotarget *7*, 42314–42329.

Cowan, C.S., Renner, M., De Gennaro, M., Gross-Scherf, B., Goldblum, D., Hou, Y., Munz, M., Rodrigues, T.M., Krol, J., Szikra, T., et al. (2020). Cell types of the human retina and its organoids at single-cell resolution. Cell *182*, 1623–1640.e34.

Deng, W.-L., Gao, M.-L., Lei, X.-L., Lv, J.-N., Zhao, H., He, K.-W., Xia, X.-X., Li, L.-Y., Chen, Y.-C., Li, Y.-P., et al. (2018). Gene correction reverses ciliopathy and photoreceptor loss in iPSC-derived retinal organoids from retinitis pigmentosa patients. Stem Cell Rep. *10*, 1267–1281.

Diakatou, M., Manes, G., Bocquet, B., Meunier, I., and Kalatzis, V. (2019). Genome editing as a treatment for the most prevalent causative genes of autosomal dominant retinitis pigmentosa. Int. J. Mol. Sci. *20*, 2542.

Dunaief, J.L. (2002). The role of apoptosis in age-related macular degeneration. Arch. Ophthalmol. *120*, 1435.

Duran Alonso, M.B., Lopez Hernandez, I., de la Fuente, M.A., Garcia-Sancho, J., Giraldez, F., and Schimmang, T. (2018). Transcription factor induced conversion of human fibroblasts towards the hair cell lineage. PLoS ONE *13*, e0200210.

Egawa, N., Suzuki, H., Takahashi, R., Hayakawa, K., Li, W., Lo, E.H., Arai, K., and Inoue, H. (2020). From in vitro to in vivo reprogramming for neural transdifferentiation: an approach for CNS tissue remodeling using stem cell technology. J. Cereb. Blood Flow Metab. *40*, 1739–1751.

Fukuda, T., Ishizawa, Y., Donai, K., Sugano, E., and Tomita, H. (2018). The poly-cistronic expression of four transcriptional factors (CRX, RAX, NEURO-D, OTX2) in fibroblasts via retro- or lentivirus causes partial reprogramming into photoreceptor cells. Cell Biol. Int. *42*, 608–614.

Furukawa, T., Morrow, E.M., and Cepko, C.L. (1997). Crx, a novel otx-like homeobox gene, shows photoreceptor-specific expression and regulates photoreceptor differentiation. Cell *91*, 531–541.

Furukawa, T., Morrow, E.M., Li, T., Davis, F.C., and Cepko, C.L. (1999). Retinopathy and attenuated circadian entrainment in Crx-deficient mice. Nat. Genet. *23*, 466–470.

Gagliardi, G., Ben M'Barek, K., Chaffiol, A., Slembrouck-Brec, A., Conart, J.-B., Nanteau, C.,

Rabesandratana, O., Sahel, J.-A., Duebel, J., Orieux, G., et al. (2018). Characterization and transplantation of CD73-positive photoreceptors isolated from human iPSC-derived retinal organoids. Stem Cell Rep. *11*, 665–680.

Grafere, T., and Enver, T. (2009). Forcing cells to change lineages. Nature *462*, 587–594.

Hasegawa, T., Ikeda, H.O., Iwai, S., Muraoka, Y., Tsuruyama, T., Okamoto-Furuta, K., Kohda, H., Kakizuka, A., and Yoshimura, N. (2018). Branched chain amino acids attenuate major pathologies in mouse models of retinal degeneration and glaucoma. Heliyon *4*, e00544.

Hohman, T.C. (2016). Hditary retinal dystrophy. Handb. Exp. Pharmacol. *242*, 337–367.

Joly, S., Francke, M., Ulbricht, E., Beck, S., Seeliger, M., Hirrlinger, P., Hirrlinger, J., Lang, K.S., Zinkernagel, M., Odermatt, B., et al. (2009). Cooperative phagocytes. Am. J. Pathol. *174*, 2310–2323.

Kanan, Y., Kasus-Jacobi, A., Moiseyev, G., Sawyer, K., Ma, J.-X., and Al-Ubaidi, M.R. (2008). Retinoid processing in cone and Müller cell lines. Exp. Eye Res. *86*, 344–354.

Kim, S.-I., Oceguera-Yanez, F., Sakurai, C., Nakagawa, M., Yamanaka, S., and Woltjen, K. (2015). Inducible transgene expression in human iPS cells using versatile all-in-one piggyBac transposons. Methods Mol. Biol. *1357*, 111–131.

Kitazawa, K., Hikichi, T., Nakamura, T., Nakamura, M., Sotozono, C., Masui, S., and Kinoshita, S. (2019). Direct reprogramming into corneal epithelial cells using a transcriptional network comprising PAX6, OVOL2, and KLF4. Cornea *38*, S34–S41.

Komuta, Y., Ishii, T., Kaneda, M., Ueda, Y., Miyamoto, K., Toyoda, M., Umezawa, A., and Seko, Y. (2016). In vitro transdifferentiation of human peripheral blood mononuclear cells to photoreceptor-like cells. Biol. Open *5*, 709–719.

Kuse, Y., Ogawa, K., Tsuruma, K., Shimazawa, M., and Hara, H. (2015). Damage of photoreceptor-derived cells in culture induced by light emitting diode-derived blue light. Sci. Rep. *4*, 5223.

Kuwahara, A., Ozone, C., Nakano, T., Saito, K., Eiraku, M., and Sasai, Y. (2015). Generation of a ciliary margin-like stem cell niche from self-organizing human retinal tissue. Nat. Commun. *6*, 6286.

Lakowski, J., Welby, E., Budinger, D., Di Marco, F., Di Foggia, V., Bainbridge, J.W.B., Wallace, K., Gamm, D.M., Ali, R.R., and Sowden, J.C. (2018). Isolation of human photoreceptor precursors via a cell surface marker panel from stem cell-derived retinal organoids and fetal retinae. Stem Cells *36*, 709–722.

Liu, H., Etter, P., Hayes, S., Jones, I., Nelson, B., Hartman, B., Forrest, D., and Reh, T.A. (2008). NeuroD1 regulates expression of thyroid hormone receptor 2 and cone opsins in the developing mouse retina. J. Neurosci. *28*, 749–756.

Mahato, B., Kaya, K.D., Fan, Y., Sumien, N., Shetty, R.A., Zhang, W., Davis, D., Mock, T., Batabyal, S., Ni, A., et al. (2020). Pharmacologic fibroblast reprogramming into photoreceptors restores vision. Nature *581*, 83–88.

Megaw, R., Abu-Arafeh, H., Jungnickel, M., Mellough, C., Gurniak, C., Witke, W., Zhang, W., Khanna, H., Mill, P., Dhillon, B., et al. (2017). Gelsolin dysfunction causes photoreceptor loss in induced pluripotent cell and animal retinitis pigmentosa models. Nat. Commun. *8*, 271.

Mellough, C.B., Collin, J., Khazim, M., White, K., Sernagor, E., Steel, D.H.W., and Lako, M. (2015). IGF-1 signaling plays an important role in the formation of three-dimensional laminated neural retina and other ocular structures from human embryonic stem cells. Stem Cells *33*, 2416–2430.

Milam, A.H., Li, Z.Y., and Fariss, R.N. (1998). Histopathology of the human retina in retinitis pigmentosa. Prog. Retin. Eye Res. *17*, 175–205.

Morrow, E.M., Furukawa, T., Lee, J.E., and Cepko, C.L. (1999). NeuroD regulates multiple functions in the developing neural retina in rodent. Development *126*, 23–36.

Nakagawa, M., Taniguchi, Y., Senda, S., Takizawa, N., Ichisaka, T., Asano, K., Morizane, A., Doi, D., Takahashi, J., Nishizawa, M., et al. (2015). A novel efficient feeder-free culture system for the derivation of human induced pluripotent stem cells. Sci. Rep. *4*, 3594.

Nakano, T., Ando, S., Takata, N., Kawada, M., Muguruma, K., Sekiguchi, K., Saito, K., Yonemura, S., Eiraku, M., and Sasai, Y. (2012). Self-formation of optic cups and storable stratified neural retina from human ESCs. Cell Stem Cell *10*, 771–785.

Oh, E.C.T., Khan, N., Novelli, E., Khanna, H., Strettoi, E., and Swaroop, A. (2007). Transformation of cone precursors to functional rod photoreceptors by bZIP transcription factor NRL. Proc. Natl. Acad. Sci. U S A *104*, 1679–1684.

Oswald, J., and Baranov, P. (2018). Regenerative medicine in the retina: from stem cells to cell replacement therapy. Ther. Adv. Ophthalmol. *10*, 251584141877443.

Parfitt, D.A., Lane, A., Ramsden, C.M., Carr, A.-J.F., Munro, P.M., Jovanovic, K., Schwarz, N., Kanuga, N., Muthiah, M.N., Hull, S., et al. (2016). Identification and correction of mechanisms underlying inherited blindness in human iPSC-derived optic cups. Cell Stem Cell *18*, 769–781.

Podda, M.V., and Grassi, C. (2014). New perspectives in cyclic nucleotide-mediated functions in the CNS: the emerging role of cyclic nucleotide-gated (CNG) channels. Pflügers Arch. *466*, 1241–1257.

Reichman, S., Slembrouck, A., Gagliardi, G., Chaffiol, A., Terray, A., Nanteau, C., Potey, A., Belle, M., Rabesandratana, O., Duebel, J., et al. (2017). Generation of storable retinal organoids and retinal pigmented epithelium from adherent human iPS cells in xeno-free and feeder-free conditions. Stem Cells *35*, 1176–1188.

Ruzycki, P.A., Zhang, X., and Chen, S. (2018). CRX directs photoreceptor differentiation by accelerating chromatin remodeling at specific target sites. Epigenetics Chromatin *11*, 42.

Schwarz, N., Lane, A., Jovanovic, K., Parfitt, D.A., Aguila, M., Thompson, C.L., da Cruz, L., Coffey, P.J., Chapple, J.P., Hardcastle, A.J., and Cheetham, M.E. (2017). Arl3 and RP2 regulate the trafficking of ciliary tip kinesins. Hum. Mol. Genet. *26*, 2480–2492.

Seko, Y., Azuma, N., Ishii, T., Komuta, Y., Miyamoto, K., Miyagawa, Y., Kaneda, M., and Umezawa, A. (2014). Derivation of human differential photoreceptor cells from adult human dermal fibroblasts by defined combinations of CRX, RAX, OTX2 and NEUROD. Genes Cells *19*, 198–208.

Seko, Y., Azuma, N., Kaneda, M., Nakatani, K., Miyagawa, Y., Noshiro, Y., Kurokawa, R., Okano, H., and Umezawa, A. (2012). Derivation of human differential photoreceptor-like cells from the Iris by defined combinations of CRX, RX and NEUROD. PLoS One *7*, e35611.

Singh, R., Cuzzani, O., Binette, F., Sternberg, H., West, M.D., and Nasonkin, I.O. (2018). Pluripotent stem cells for retinal tissue engineering: current status and future prospects. Stem Cell Rev. Rep. *14*, 463–483.

Swaroop, A., Kim, D., and Forrest, D. (2010). Transcriptional regulation of photoreceptor development and homeostasis in the mammalian retina. Nat. Rev. Neurosci. *11*, 563–576.

Takahashi, K., and Yamanaka, S. (2006). Induction of pluripotent stem cells from mouse embryonic and adult fibroblast cultures by defined factors. Cell *126*, 663–676.

Tu, H.-Y., Watanabe, T., Shirai, H., Yamasaki, S., Kinoshita, M., Matsushita, K., Hashiguchi, T., Onoe, H., Matsuyama, T., Kuwahara, A., et al. (2019). Medium- to long-term survival and functional examination of human iPSC-derived retinas in rat and primate models of retinal degeneration. EBioMedicine *39*, 562–574.

Wahlin, K.J., Maruotti, J.A., Sripathi, S.R., Ball, J., Angueyra, J.M., Kim, C., Grebe, R., Li, W., Jones, B.W., and Zack, D.J. (2017). Photoreceptor outer segment-like structures in long-term 3D retinas from human pluripotent stem cells. Sci. Rep. *7*, 766.

Wheway, G., Nazlamova, L., Turner, D., and Cross, S. (2019). 661W photoreceptor cell line as a cell model for studying retinal ciliopathies. Front. Genet. *10*, 308.

Xiang, M. (2013). Intrinsic control of mammalian retinogenesis. Cell. Mol. Life Sci. *70*, 2519–2532.

Zhang, K., Liu, G.-H., Yi, F., Montserrat, N., Hishida, T., Esteban, C.R., and Izpisua Belmonte, J.C. (2014). Direct conversion of human fibroblasts into retinal pigment epithelium-like cells by defined factors. Protein Cell *5*, 48–58.

Zhou, Q., Brown, J., Kanarek, A., Rajagopal, J., and Melton, D.A. (2008). In vivo reprogramming of adult pancreatic exocrine cells to β-cells. Nature *455*, 627–632.

STAR★METHODS

KEY RESOURCES TABLE

REAGENT or RESOURCE	SOURCE	IDENTIFIER
Antibodies		
Mouse monoclonal anti-CNG Channel	GeneTex	Cat#GTX79456; RRID: AB_11167547
Rabbit polyclonal anti-CONE ARRESTIN	Merck Millipore	Cat#AB15282; RRID: AB_1163387
Goat polyclonal anti-NRL	R&D systems	Cat#FNK-AF2945; RRID: AB_2155098
Rabbit polyclonal anti-RECOVERIN	ProteinTech	Cat#10073-1-AP; RRID: AB_2178005
Mouse monoclonal anti-RHODOPSIN	Sigma Aldrich	Cat#O4886; RRID: AB_260838
Goat anti-rabbit Alexa- 488	Thermo Fisher Scientific	Cat#A11034
Goat anti-mouse Alexa- 488	Thermo Fisher Scientific	Cat#A11029
Goat anti-mouse Alexa- 594	Thermo Fisher Scientific	Cat#A11032
Donkey anti-goat Alexa- 594	Thermo Fisher Scientific	Cat#A11058
Chemicals, peptides, and recombinant proteins		
Doxycycline	TAKARA	Cat#631311
9-cis-Retinal	Cayman	Cat#21692
N-acetylcysteine	Wako	Cat#015-05132
Z-VAD-FMK	Peptide Institute	Cat#3188-v
Critical commercial assays		
miRNeasy Mini Kit (50)	QUIAGEN	Cat#217004
SuperScript™ VILO™ MasterMix	Thermo Fisher Scientific	Cat#11755050
TaqMan® Gene expression Master Mix	Thermo Fisher Scientific	Cat#4369016
Lipofectamine LTX Reagent	Thermo Fisher Scientific	Cat#15338100
Pluronic F-127	Sigma-Aldrich	Cat#P2443
Fluo-8 AM	AAT Bioquest	Cat#21080
8-Br-cGMP	Sigma-Aldrich	Cat#B1381
Deposited data		
Single-cell RNA sequencing data	This paper, deposited at NBDC/GEA	J-DS000586
Experimental models: Cell lines		
Human iPSCs	RIKEN BioResource Research Center	HPS1042 HPS1749 HPS0063
Human ESCs	WiCell	H9
Recombinant DNA		
KW110_PB_TA_ERN (Ef1a_rtTA_neo) vector	Kim et al., 2015	Addgene; Plasmid #80474

RESOURCE AVAILABILITY

Lead contact

Further information and requests for resources and reagents should be directed to and will be fulfilled by the lead contact, Haruhisa Inoue (haruhisa.inoue@riken.jp).

Materials availability

Antibodies, and other reagents used in this study were commercially available, and company and catalog numbers were provided in supplemental information. Plasmids generated on this study are available from the corresponding author on request.

Data and code availability

- Single-cell RNA sequencing data have been deposited at National Bioscience Database Center (NBDC) and Genomic Expression Archive (GEA) under application number J-DS000586 (https://biosciencedbc.jp/en/).
- This study did not generate novel computer code/ software.
- Any additional information required to reanalyze the data reported in this paper is available from the lead contact upon request.

EXPERIMENTAL MODEL AND SUBJECT DETAILS

iPS and ES cell lines and maintenance

The use of iPSCs and ESCs was approved by the Ethics Committees of RIKEN BioResource Research Center and department of Medicine and Graduate School of Medicine of Kyoto University. The data on human iPSCs and ESCs used in the present study are shown in Table S1. Human iPSCs were maintained on laminin (iMatrix-511; TAKARA, Kusatsu, Japan) in StemFit AK02N medium (Ajinomoto, Tokyo, Japan) at 37°C in a standard 5% CO_2 incubator, according to a published protocol (Nakagawa et al., 2015), with slight modifications. Passages were performed every seventh day. Prior to passaging, culture plates were coated with laminin in phosphate buffered saline (PBS) at 37°C for at least one hour. iPSC colonies were treated with TrypLE Select Enzyme (Thermo Fisher Scientific, Waltham, MA) at 37°C for four minutes (min) and dissociated into single cells by gentle pipetting. The dissociated iPSCs were suspended in StemFit medium and counted with Countess II Automated Cell Counter (Thermo Fisher Scientific). The single-cell iPSC suspension was plated at a density of 13,000 cells per well and cultured in StemFit medium with 10 μM Y-27632 Rock inhibitor (Nacalai-Tesque, Kyoto, Japan). The medium was changed to StemFit without Y-27632 on the following day and then further changed every other day. ESCs were cultured as well as iPSCs.

METHOD DETAILS

Preparation of a *piggyBac* vector and introduction into iPSCs

Polycistronic vectors were generated, containing murine cytomegalovirus (mCMV) promoter, CRX and NEUROD1 under control of the tetracycline operator rtTA and neomycin resistance gene with the KW110_PB_TA_ERN (Ef1a_rtTA_neo) vector backbone (Kim et al., 2015). The plasmid was gifted from Knut Woltjen (Addgene plasmid # 80474). For transfection purpose, iPSCs were seeded on laminin coated 6-well plates at a density of 13,000 cells per well. The cells were grown for three days and transfected with 1.75 μg of DNA using Lipofectamine LTX Reagent (Thermo Fisher Scientific) according to the manufacturer's instructions. The following day, culture medium was changed to StemFit medium. After clone selection using neomycin (G418 Sulfate; Sigma-Aldrich, St. Louis, MO), stable iPSC and ESC clones were established.

Photoreceptor-like cell differentiation from human iPSCs

For differentiation toward photoreceptor-like cells, we used differentiation media based on the previous reports (Kuwahara et al, 2015), containing DMEM/F12 - Glutamax (Thermo Fisher Scientific), 1% N2 supplement (Thermo Fisher Scientific), 10% Fetal Bovine Serum (FBS; Thermo Fisher Scientific), 0.5 μM RA (Sigma-Aldrich), and 0.1 mM taurine (Sigma-Aldrich). CRX and NEUROD1 introduced iPSCs were dissociated with TrypLE Select and plated on laminin-coated 6-well plates at a density of 150,000 cells per well, with the medium containing 10 μM Y-27632. At this point, 1 μg/ml doxycycline (TAKARA) was added to the medium until three days before any analysis. After overnight incubation, the medium was changed to fresh medium without Y-27632, and half of the medium was changed every 2-3 days. ESCs were differentiated as well as iPSCs.

For the formation of 3D structure, iPSCs were dissociated into single cells in TrypLE select and re-aggregated using low-cell adhesion 96-well plates with V-bottomed conical wells (Sumilon PrimeSurface plate; Sumitomo Bakelite, Tokyo, Japan) in differentiation medium (12,000 cells per well, 100 μl) supplemented with 20 μM Y-27632 under 5% CO_2 at 37°C (defined as day 0). On culture day 3, 50 μL medium was added to the culture. From day 5, half of the medium was changed every 2-3 days.

Reverse transcription quantitative polymerase chain reaction (RT-qPCR)

Total RNAs were extracted using RNeasy PlusMini Kit (QIAGEN, Hilden, Germany) according to the manufacturer's protocol. RNA yields and quality were checked with a NanoDrop spectrophotometer (Thermo

Fisher Scientific). Complementary DNA (cDNA) was synthesized from 2 μg of mRNA using SuperScript™ VILO™ MasterMix (Thermo Fisher Scientific) following the manufacturer's recommendations. Synthesized cDNA was diluted at 1/9 in DNase-free water before performing quantitative PCR. qPCR analysis was performed on QuantStudio™ 12K Flex Real-Time PCR System (Thermo Fisher Scientific) with custom TaqMan® Array 96-Well Fast plates and TaqMan® Gene expression Master Mix (Thermo Fisher Scientific) according to the manufacturer's instructions. All primers and Minor Groove Binder (MGB) probes labeled with fluorescein (FAM) for amplification were purchased from Thermo Fischer Scientific (Table S2). Results were normalized against glyceraldehyde-3-phosphate dehydrogenase (GAPDH), and quantification of gene expression was based on the Delta Delta Ct Method in three independent biological experiments.

Immunocytochemistry (ICC)

Cells were fixed in 4% paraformaldehyde (PFA) for 15 min at room temperature, washed with PBS and permeabilized in PBS containing 0.2% Triton X-100 for 30 min at room temperature, and incubated with block reagent (Block Ace; Yukijirushi, Tokyo, Japan). After incubation with primary antibodies overnight at 4°C, cells were washed three times with PBS and incubated with appropriate secondary antibodies for one hour at room temperature. Cell images were acquired with FLUOVIEW FV3000 (Olympus Life Science, Tokyo, Japan) or IN Cell Analyzer 6000 (GE Healthcare, Chicago, IL). The numbers of cells were quantified with IN Cell Analyzer 6000 and IN CELL Developer toolbox software 1.9. The primary antibodies used in this assay were listed in Table S3.

The immunostaining procedure for the 3D structure was performed by the following steps. Aggregates were fixed with 4% PFA for 15 min at room temperature and incubated in 30% sucrose in PBS overnight at 4°C for cryo-protection. The fixed aggregates were embedded in OCT compound (Sakura Finetek, Tokyo, Japan) and stored at -80°C. Cryo-sections of 12 μm thickness were made with a Cryostat (Leica, Wetzlar, Germany). Samples were permeabilized with 0.3% Triton X-100 in PBS-T (PBS with 0.1% Tween 20) for 15 min and incubated with block buffer for one hour at room temperature. They were incubated with primary antibodies dilated in blocking buffer at 4°C overnight, followed by incubation with secondary antibodies conjugated with Alexa 488, 594 and DAPI at room temperature for one hour.

Single-cell RNA sequencing

Two dimensional iPRCs on day 28 were collected with Accumax Cell/Tissue Dissociation Solution (Lagen Laboratories, Rochester, MI) at 37°C for 10 min. The dissociated cells were suspended in PBS containing 10 μM Y-27632 and 0.1% BSA, which was then immediately followed by a library preparation targeting single cells using the Chromium Next GEM Single Cell 3' Reagent Kits v3.1 (10×Genomics, CA) according to the manufacturer's instructions. Six thousand cells were analyzed, and the library was sequenced on NovaSeq 6000 (Illumina, San Diego, CA). Cell-specific FASTQ files were generated by deconvolution of UMIs and cell barcodes using bcl2fastq 2.20.0.422 (Illumina). Alignment to the human reference genome GRCh38 and UMI counting were conducted by Cell Ranger v6.1.1 pipeline (10×Genomics). Data analysis including t-distributed Stochastic Neighbor Embedding (tSNE) were implemented in the Seurat package v3.2.3.

Calcium imaging

For functional analysis, iPRCs on day 21 were collected using Accumax Cell/Tissue Dissociatetion Solution at 37°C for five min and dissociated into single cells by gentle pipetting. The dissociated cells were suspended in the differentiation medium with 10 μM Y-27632, counted and plated on laminin-coated μ-dish (ibidi, GmbH, Gräfelfing, Germany) at a density of 200,000 cells in 100 μL per dish. The medium was changed to differentiation medium without Y-27632 on the following day and doxycycline was removed on day 25.

After PBS wash, iPRCs on day 28 were exposed to differentiation medium containing 0.05 % Pluronic F-127 (Sigma-Aldrich) and 5 μm Fluo-8 AM (AAT Bioquest, Sunnyvale, CA) at 37°C for 30 min. Cells were washed with PBS three times and changed to Neurobasal Minus Phenol Red (Thermo Fisher Scientific). Fluorescence intensity of iPRCs was monitored using Nikon A1R MP microscopy (Nikon, Tokyo, Japan). As control, the medium without cGMP analogue was applied and the trace of fluorescence was recorded. For each measurement, 30-second baseline activity was recorded before cGMP analogue (8-Br-cGMP; Sigma-Aldrich) was added at a final concentration of 100 μM. Fluorescence change was analyzed with NIS-Elements AR Analysis software using the formula of $\Delta f / f$, where f was the average cellular fluorescence during baseline activity and Δf was the change from baseline fluorescence.

Light-induced cell death analysis

Differentiated cells were replated into laminin-coated 24-well plates at a density of 50,000 cells per well on day 14. After overnight incubation, the medium was changed to fresh medium without Y-27632. Half of the medium was changed every 2-3 days and doxycycline was removed on day 25. On day 27, the medium was changed to DMEM/F12, no phenol red (Thermo Fisher Scientific) supplemented with 1% N2 supplement, 0.5 μM RA, 0.1 mM taurine to prevent nutrients from degrading. To activate the phototransduction cascade, 9-cis-Retinal vitamin A analog (Cayman Chemical, Michigan, CA) was added to the media four hours before light exposure (final concentration: 10 μM). After iPRCs were treated with *N*-acetylcysteine (NAC) (Wako, Osaka, Japan) or 25μM Z-VAD-FMK (Peptide Institute、Osaka, Japan) or vehicle (phenol free DMEM), the cells were incubated for 1 hour. The cells were then exposed to 10,000 lux white LED light under 5% CO_2 at 37°C for 24 hours. Dark control cells were all from the same stock and were cultured simultaneously in another incubator. We confirmed that medium temperature did not affect the cell viability by thermometer measurements. Following light exposure, cells were fixed in 4% PFA for immunostaining.

QUANTIFICATION AND STATISTICAL ANALYSIS

We conducted the experiments with biological triplicates and data are expressed as mean ± standard error of mean (SEM). Results were analyzed using one-way analysis of variance (ANOVA) followed by Dunnett's post hoc test or unpaired t-test to determine statistical significances of the data. All analyses were performed using statistical software (SPSS Statistics 19; SPSS, Inc., Chicago, IL), and statistical significance was defined as $p < 0.05$.